

# Sub-cycle Event Detection and Characterization in Continuous Streaming of Synchro-waveforms: An Experiment Based on GridSweep Measurements

Narges Ehsani, *Student Member, IEEE*, Fatemeh Ahmadi-Gorjayi, *Student Member, IEEE*, Zong-Jhen Ye, *Student Member, IEEE*, Alex McEachern, *Life Fellow, IEEE*, and Hamed Mohsenian-Rad, *Fellow, IEEE*

**Abstract**—Continuous streaming of *synchro-waveforms*, i.e., time-synchronized waveform measurements, can provide a comprehensive record of the status of the power system. The key to unmask the value of such massive data recording is to extract the most informative aspects of the data. In this paper, we develop and test new methods to detect and characterize *sub-cycle* events in continuous streaming of synchro-waveforms. The measurements in this study are collected by the authors in a practical test-bed in California. The measurements are made at low-voltage circuits under two different substations, using GridSweep devices with GPS time stamping. Over 40 billion data points were collected during one month. Several practical challenges are addressed, including the computational complexity due to the enormous size of data, the need for realignment between waveform samples and cycles, and the challenges in extracting differential waveforms to reveal the event signatures.

**Keywords:** Synchro-waveforms, waveform measurement unit, GridSweep, continuous waveform data streaming, event detection, sub-cycle event, system-wide event, differential waveform.

## I. INTRODUCTION

Synchro-waveform is an emerging concept in power system monitoring and situational awareness. It refers to *time-synchronized* voltage and/or current *waveform* measurements from multiple locations in power system, e.g., see [1], [2].

The device to measure synchro-waveforms is referred to as Waveform Measurement Unit [3, Section 4-6]. WMUs measure and time-stamp the raw waveforms; therefore, they can provide more details about various events and abnormalities in power systems, compared to Phasor Measurement Units (PMUs). WMUs can help reveal a wide range of waveform events and abnormalities that are typically missed by PMUs, due to the short duration or the small magnitude of the event.

### A. Approach and Contributions

In this paper, our focus is on a new frontier in the analysis of synchronized waveform data, namely the *continuous streaming* of synchro-waveforms. This is also sometimes referred to as time-synchronized *Continuous Point-on-Wave* (CPOW) measurements in the literature; e.g., see [4], [5].

Although this is a promising new area, the limited access to real-world synchro-waveform streaming poses a research challenge. The authors have addressed this obstacle by utilizing a



Fig. 1. One of the four GridSweep devices that was used in this study.

new device, called GridSweep [6], see Fig. 1, to obtain one month of continuous streaming of synchro-waveforms at low-voltage circuits at *multiple* locations in Riverside, CA. The details of the experiments are explained in Section II.

Our focus in this paper is on *event detection* and *event characterization*. To the best of our knowledge, this is the first study that addresses these two tasks based on *real-world* continuous streaming of synchro-waveform data from *multiple* locations on low-voltage circuits over a *long period* of time.

The practical nature of this study unmasks several real-world challenges, ranging from the samples not being aligned with waveform cycles or the computational challenges of working with an enormous amount of waveform data.

Another key aspect of our work is its emphasis on capturing and analyzing *sub-cycle* events, i.e., the events that last less than one AC cycle. We study and characterize such events based on coordinated analysis of time-synchronized waveform data from four GridSweep devices at low-voltage circuits, and one utility-grade three-phase waveform sensor at a substation.

### B. Literature Review

Continuous streaming of synchro-waveforms is generally a new concept. Doing it in low-voltage circuits is also particularly new. In fact, to the best of our knowledge, GridSweep is the first device that provides continuous streaming of synchro-waveforms at regular 120 V power outlets. However, so far, the primary application of GridSweep has been on steady-state analysis, such as low-voltage probing over several minutes to hours [6], or the analysis of harmonics/inter-harmonics [7].

In this paper, our focus is rather on detecting and characterizing *transient events* in the continuous streaming of synchro-waveforms from GridSweep devices. We are interested in not only the events that are captured by a *single* GridSweep device, but also those events that have regional or system-wide impacts and are captured by *multiple* GridSweep devices.

N. Ehsani, F. Ahmadi-Gorjayi, Z. J. Ye, and H. Mohsenian-Rad are with the University of California, Riverside, CA, USA. A. McEachern is with McEachern Laboratories, Alameda, CA, USA. Zong-Jhen Ye and Fatemeh Ahmadi-Gorjayi contributed *equally* to this work. The corresponding author is Hamed Mohsenian-Rad. E-mail: hamed@ece.ucr.edu.

When it comes to the first type of events, i.e., the analysis of waveform measurements from one sensor at one location, the relevant literature includes [8]–[12]. In [8], an abnormality detection is done based comparing the statistical distributions of the variations in the current waveforms that are measured by power quality sensors. In [12], deep auto-encoder is used to build an event identification method over the harmonic distortion data. A common approach in the literature is to apply the proposed methods to waveforms that are generated by a Real-Time Digital Simulator (RTDS); such as in [10]. For the methods that use real-world data, the focus is waveform data for events that are previously detected by power quality or fault sensors from utility substations; such as in [9].

The new field of synchro-waveforms has started to emerge only recently. We are not aware of any study in this domain that works with continuous streams of real-world synchro-waveforms; due to lack of access to such time-synchronized data streams. Instead, the existing literature has only showed some examples of such events; again with focus on measurements at high-voltage and medium-voltage circuits; e.g., see [1], [13], [14]. On the contrary, in this paper, we do a comprehensive analysis of such events using continuous steaming of synchro-waveform data from GridSweep devices.

## II. SETUP OF THE EXPERIMENT

Fig. 2 shows the setup of our experiments in Riverside, CA. Four GridSweep devices are used in this study, plugged into 120 V power outlets to measure voltage waveforms at their respective locations. They are denoted by WMU 1, WMU 2, WMU 3, and WMU 4. WMU 1 is plugged into a power outlet on Phase A. Through multiple transformers (12.47 kV / 480 V and 480 V / 120 V), the outlet at this location is connected to a 12.47 kV power distribution feeder, served by Substation 1. WMUs 2, 3, and 4 are *individually* plugged into three different power outlets that are three different phases (Phases A, B, and C) in another building, about two miles away from the location of WMU 1. The building where WMU 2, 3, and 4 are located is served by a 12.47 kV power distribution feeder, through Substation 2. Substation 1 and Substation 2 are connected to each other through a 69 kV transmission line.

Each GridSweep records single-phase voltage waveform at a sampling rate of 4.3 kHz, i.e., roughly 72 to 73 samples per cycle. Each device is equipped with a GPS signal receiver with precise pulse per second (PPS) capability. The PPS pulses at the beginning of each GPS clock second. The pulse is marked on the data stream to time-stamp the waveform measurements.

The period of this study was from October 1 till October 31, 2022. A total of roughly 11 billion ( $4.3 \times 60 \times 60 \times 24 \times 30$ ) samples were recorded per device during this period.

This study also included an industry-grade WMU at Substation 2, namely a three-phase SEL power quality meter. It is marked as WMU 5 in Fig. 2. WMU 5 is capable of capturing major events in the power system using an *event-triggered* mechanism. We will use data from WMU 5 in Section V to gain additional insight about the system-wide events that are observed by all the WMUs in this study. Importantly, WMU 5 has a higher sampling rate at 7.68 kHz, i.e., 128 samples

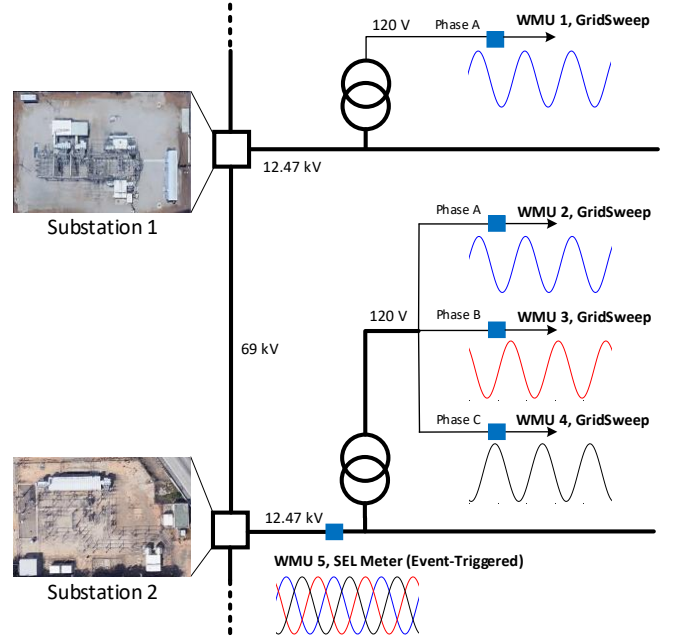


Fig. 2. The setup of the experiments in Riverside, CA. Four GridSweep devices are used to stream synchro-waveforms from two buildings that are served by different substations. The GridSweep devices serve as four WMUs, marked as WMUs 1, 2, 3, and 4. A utility-grade three-phase SEL power quality meter is available at Substation 2 to serve as an event-triggered WMU.

per cycle. However, it is common for WMU 5 to miss some of the events that are observed by the rest of the WMUs.

Note that, GridSweep devices provide continuous waveform data streaming; therefore, there is no concern in missing any event with WMUs 1, 2, 3, and 4; as long as we can detect the event. This is the topic of our discussion in Section III.

Throughout this paper, an “event” is defined as any anomaly in voltage waveforms. Since GridSweep is installed at low voltage circuits, the events that it captures may have diverse root causes, such as local events that are visible only on the same distribution feeder, or system-wide events that are visible across the sub-transmission system or the transmission system.

## III. EVENT DETECTION

Given the extremely large volume of data in the continuous streaming of synchro-waveforms, event detection must be done by methods that have *light-weight* computational complexity. Accordingly, in this paper, we use *total harmonic distortion* (THD) [15] as the quantity to help us with event detection. In this regard, we seek to answer two questions: 1) Over *what window of time* we should calculate THD to detect an event in the stream of voltage waveforms? 2) What *practical issues* may arise when we work with real-world waveform data that may affect the performance of event detection, and how can we address them to achieve reliable event detection results?

### A. Event Detection based on THD

A waveform *event* is often manifested in form of a *waveform distortion*. Let  $\text{THD}_{\text{present}}$  denote the present calculation of THD. Similarly, let  $\text{THD}_{\text{prior}}$  denote the prior calculation of THD. We detect an event when the following inequality holds:

$$\Delta\text{THD} = |\text{THD}_{\text{present}} - \text{THD}_{\text{prior}}| \geq \alpha, \quad (1)$$

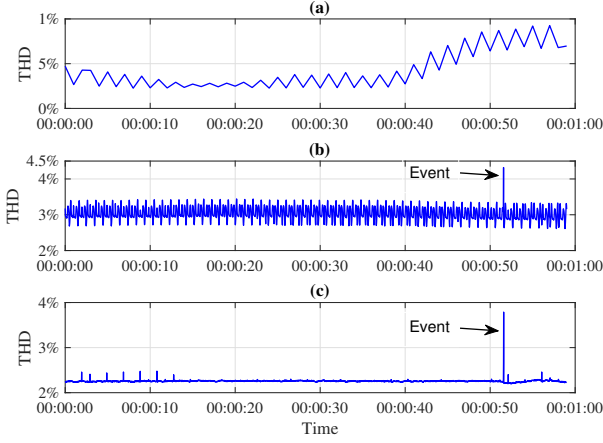


Fig. 3. THD calculation for one minute of voltage waveforms: (a) per-second THD; (b) per-cycle THD using the original waveform samples; (c) per-cycle THD using up-sampled waveform with better sample-to-cycle alignment.

where  $\alpha$  is a parameter act as the threshold for event detection. Notice that, what matters here is the *change* in THD; not the actual value of THD itself. In fact, THD could take any value depending on the presence of steady-state background harmonics in the system. Regarding the choice of detection threshold  $\alpha$ , it can act as a knob to control the level of sensitivity in event detection; e.g., see [3, Section 4.2.1].

Traditionally, THD is considered a long-term factor, which is calculated over a long period of time, such as one hour. Per IEEE Standard 519-2014, the shortest interval over which THD is calculated is three seconds. However, when it comes to event detection in waveform measurements, THD must be calculated in much smaller time frames in order to be useful. Next, we discuss this issue and the challenges that it may arise in a practical event detection task in synchro-waveforms.

### B. Per-Second vs Per-Cycle THD Analysis

A much shorter time-frame is to calculate THD once every second. Fig. 3(a) shows an example for *per-second* THD calculations based on GridSweep data over a period of one minute. Next, consider the *per-cycle* THD values in Fig. 3(b) that are obtained by using the exact same data set during the exact same one minute. In total, 3600 ( $60 \times 60$ ) per-cycle THD values are calculated in this figure (at 60 Hz AC power system). Here, we can see a *sudden jump* in the THD value at time 00:00:53. Interestingly, there was no indication of any such jump in the per-second THD values in 3(a). The reason is that the event in this example was a *sub-cycle* event, i.e., it lasted for one cycle or less. The impact of such sub-cycle event cannot be seen in the per-second THD values in 3(a). We must instead check the per-cycle THD values in 3(b).

Therefore, throughout this paper, we use per-cycle THD values for the purpose of event detection in synchro-waveforms.

### C. Impact of Samples Not Being Aligned with Cycles

Next, consider the THD values in Fig. 3(c). This figure too is based on per-cycle THD calculation. The THD values shown in Fig 3(b) and Fig 3(c) are calculated from exactly the same continuous synchro-waveforms. But in the Fig 3(c), the

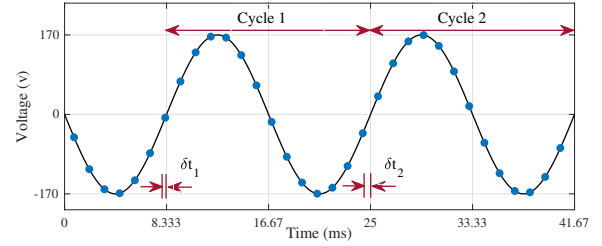


Fig. 4. Conceptual illustration (not from real data) of the lack of alignment between the measurement *samples* and the waveform *cycles*. Even though the samples have fixed time-intervals, they are not aligned to the cycles.

waveform samples are up-sampled prior to THD calculation. The results are much more smooth. In fact, the presence of the event is much more evident in Fig. 3(c) than in Fig. 3(b).

To understand the reasons behind the better results in Fig. 3(c), let us consider the waveform in Fig. 4. To accurately compute per-cycle THD, individual full cycles must be examined. This necessitates identifying two data points that mark the start and end of each cycle. However, when sampling points are *not* aligned with the cycles, it becomes impossible to have equal number of samples in each cycle. Here, the time offset of the first available sample in each cycle with respect to the true start of the cycle is defined as  $\delta t$ . Accordingly,  $\delta t[c]$  is the time offset corresponding to cycle  $c$ . Since the sampling rate of GridSweep is not an integer multiple of fundamental frequency (i.e. 60 Hz), the samples are *not* precisely aligned with the cycles. Therefore, in practice, we almost always have:

$$\delta t[c_1] \neq \delta t[c_2] \neq 0, \quad (2)$$

where  $c_1$  and  $c_2$  are two consecutive cycles in the measured waveform. Misalignment between samples and cycles can happen also because of the variations in power system frequency. This too can lead to sample-to-cycle-misalignment. Samples that are not aligned with cycles result in some *residues* from neighboring cycle in the calculation of the *per-cycle* THD. This is the main reason behind the *fluctuations* in Fig. 3(b). This issue is amplified, particularly, when the sampling rate per cycle is relatively low. Therefore, up-sampling can mitigate the problem by bringing the values of  $\delta t[c]$  close to zero.

Fig. 3(c) presents a much smoother per-cycle THD profile for the same time period, achieved by up-sampling the raw waveform (originally with  $72 \sim 73$  samples per cycle) to 512 samples per cycle. Up-sampling is done in MATLAB using command *resample* [16] over waveforms of length one second with input parameters 4300 (sampling rate of the original waveform) and 30,720 (sampling rate of the upsampled waveform).

Although up-sampling is a remedy to reduce the fluctuations in the per-cycle THD calculations, it significantly adds to the computational burden. Considering the large volume of the dataset, we have opted not to use up-sampling as part of event detection. Instead, we use a similar approach *after* an event is detected to resolve the impact of sampling not being aligned with cycles to characterize the event; see Section IV-B.



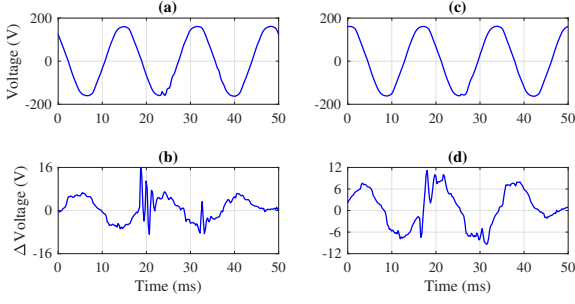


Fig. 5. Two examples for single-phase events: (a) raw voltage waveform of the first event; (b) the corresponding differential waveform; (c) raw voltage waveform of the second event; (d) the corresponding differential waveform.

#### IV. DIFFERENTIAL WAVEFORM ANALYSIS

When it comes to sub-cycle events in waveform measurements from low-voltage circuits, it is often difficult to characterize the event by looking at the raw waveform. Two examples are shown in Figs. 5(a) and 5(c). Notice that, the event is very minor compared to the main steady-state waveforms. To tackle this issue, we rather focus on analyzing *differential waveforms*.

##### A. Differential Waveform Extraction

Consider a raw voltage waveform  $v(t)$  from measurements. The *differential waveform* corresponding to  $v(t)$  is defined as:

$$\Delta v(t) = v(t) - v(t - NT), \quad (3)$$

where  $T$  is the waveform interval, i.e.,  $T = 1/60$  second for a 60 Hz waveform; and  $N$  is a small integer number, such as 1, 2, 3, 4, or 5; see [3, pp. 151-152]. Here,  $v(t - NT)$  serves as a *reference* for the “normal” waveform *before* the event happens. In this regard, the subtraction in (3) can approximately remove the normal portion of the waveform, leaving only the abnormality that was *superimposed* to the normal waveform due to the occurrence of the event<sup>1</sup>.

Fig. 5(b) shows the differential waveform corresponding to the raw waveform in Fig. 5(a). Also, Fig. 5(d) shows the differential waveform corresponding to the raw waveform in Fig. 5(c). We see that the event is much better represented in the differential waveform than in the raw waveform. Yet, there are still some considerable *residue* from the normal waveform in the differential waveforms, specially in Fig. 5(d).

##### B. Remedy: Cycle-Aligned Sample Interpolation

To reduce the residue in differential waveforms, we first need to understand the root cause of the problem. The issue here is again the *lack of alignment* between the sampling time and the waveform cycles, as we also saw in Fig. 4.

Here, the challenge is that we *cannot* exactly align each sample of  $v(t)$  to its corresponding sample in  $v(t - NT)$  in order to correctly obtain  $\Delta v(t)$  as in (3). To resolve this issue, we need to estimate the value of the *properly aligned* sample in  $v(t - NT)$ . This can be done using *interpolation*. The idea is shown in Fig. 6. Consider the sample that is marked with a red arrow. In order to obtain the differential waveform, we need to subtract this sample from the sample that is exactly

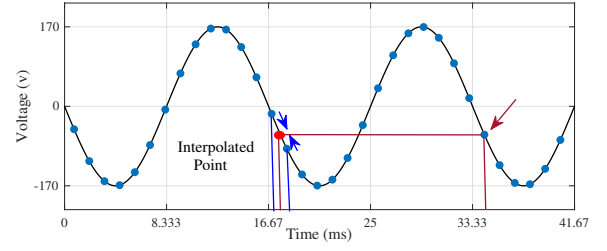


Fig. 6. Conceptual illustration (not from real data) of using interpolation to resolve the lack of alignment between *samples* and *cycles*, while extracting the differential waveform. Here, we first interpolate  $v(t - T)$  and then subtract it from a given sample at  $v(t)$  to obtain  $\Delta v(t)$  using (3), where  $N = 1$ .

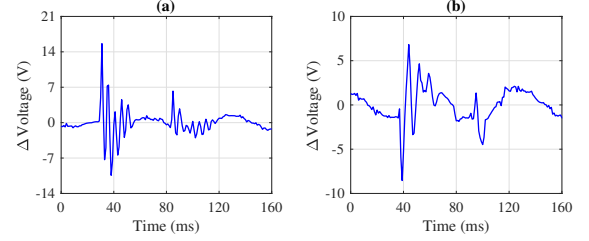


Fig. 7. The results after using interpolation. Single-phase at WMU 1.

$NT$  seconds before this sample. However, since the sampling times are not aligned with the waveform cycles, there is *no* such available. Therefore, we estimate the value of the missing sample by using an interpolation of the two samples that are closest in time, before and after the missing sample.

Interpolation is done in MATLAB using command *interp1* with *spline* interpolation [18]. The results are shown in Figs. 7(a) and (b), respectively. Comparing these new results with those in Figs. 5(b) and 5(d), we can see that the latter differential waveforms extract the event signatures more clearly.

##### C. Three-Phase Events at WMUs 2, 3, and 4

Recall from Section II that WMUs 2, 3, and 4 are plugged in to power outlets that are on three different phases. Accordingly, the continuous synchro-waveforms that are streamed from these three WMUs can allow monitoring voltage on all three phases. Accordingly, we can simultaneously conduct event detection on all three phases. Cycle-alignment can also be done based on applying sample interpolation on each phase.

Here, we are particularly interested in the events that affect all the three phases. Two such events are shown in Figs. 8 and 9. First, consider the example in Fig. 8(a), which shows the raw waveforms, Fig. 8(b) shows the corresponding differential waveforms. We can see two distinct instances of oscillations on all the three phases. Each instance takes less than half a cycle. Next, consider the example in Fig. 9(a), which shows the raw waveforms. Fig. 9(b) shows the corresponding differential waveforms. Again, we can see two distinct sub-cycle periods of oscillations in the voltage waveforms on all the three phases.

Even though the transient event in Fig. 9 is less severe than the transient event in Fig. 8, it appears that these two three-phase events generally follow the same patterns. It is possible that these two events are the repetition of the same physical phenomena. Identifying such similarities can sometimes has applications in *condition monitoring* or identifying *incipient failures* in power systems; see [3, Section 4.3].

<sup>1</sup> A concept similar to differential waveform but with a different terminology is called *cycle-delayed* waveform, e.g., see [17].

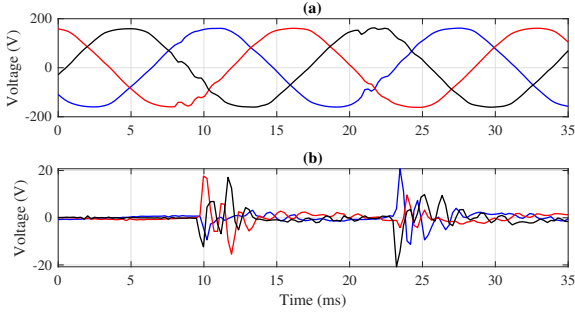


Fig. 8. The first example for a three-phase event, i.e., an event that affects all three phases: (a) raw voltage waveforms; (b) differential voltage waveforms.

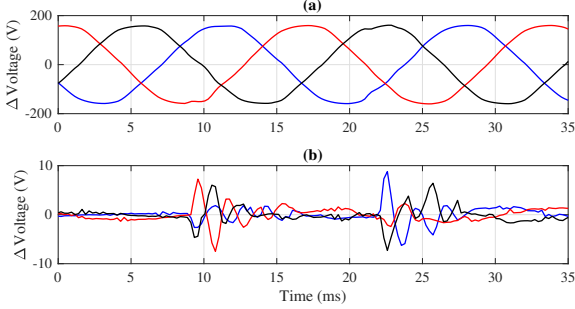


Fig. 9. The second example for a three-phase event; which is less severe than the first example in Fig. 8, yet it still affects all the three phases: (a) raw voltage waveforms; (b) differential voltage waveforms.

## V. SYSTEM-WIDE EVENTS IN SYNCHRO-WAVEFORMS

So far, our analysis was focused on investigating the events at each location separately. However, since GridSweep devices provide time-synchronized measurements using GPS signals, we can use the data to detect and characterize the system-wide events in the power system, i.e., those events that are visible at *multiple* power distribution feeders on the power system.

### A. Detecting System-Wide Events

In order to detect system-wide events, we need to align and compare the event detection task across multiple locations in the power system. Fig. 10 shows how this process works.

First, consider the values of  $\Delta\text{THD}$  in Fig. 10(a) that are extracted at WMU 1 in a period of two minutes, from 06:09:00 till 06:11:00. Recall that WMU 1 is served by Substation 1; see Fig. 2. Two events are flagged during this period, at 06:09:07 and at 06:10:24. Next, consider the values of  $\Delta\text{THD}$  in Fig. 10(b) that are extracted at WMU 2 during the exact same period. Recall that WMU 2 is served by Substation 2; see Fig. 2. One event is flagged during this period, at 06:10:24.

The event at 06:09:07 at WMU 1 was a *local* event; because it was observed only in one location. However, the event at 06:10:24 at WMU 2 was a *system-wide* event (i.e., a non-local event); because it was observed not only at WMU 1 under Substation 1 but also at WMU 2 under Substation 2. Identifying such sub-cycle yet system-wide events is one of the key advantages of using precise time synchronization in waveform measurements; see [1] for some related discussions.

### B. Overview of Synchronized Events

By following the approach in Section V-A, we identified 26 system-wide events across WMU 1 and WMU 2, which

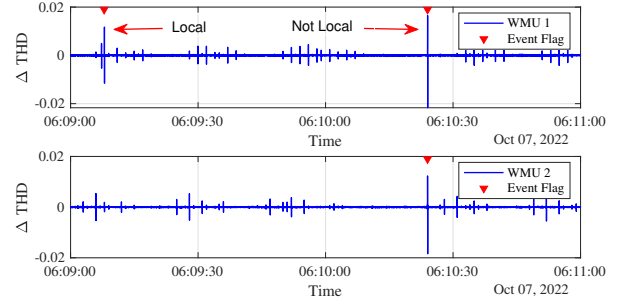


Fig. 10. Identifying and separating system-wide events from local events by comparing the  $\Delta\text{THD}$  profiles at WMU 1 (under Substation 1) and WMU 2 (under Substation 2). Here, one system-wide event is detected at 06:10:24.

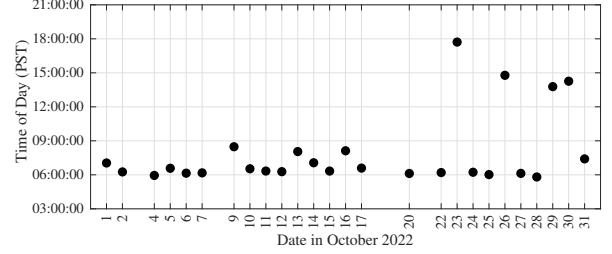


Fig. 11. Timing of the detected system-wide oscillatory events.

generally had similar patterns, involving oscillations. The timing of these 26 system-wide events are shown in Fig. 11. Out of the total 31 days of this study, this particular system-wide event was not present on 5 days. We never observed more than one system-wide event of this type on one day.

The majority of the events happened between 6:00 AM and 9:00 AM. In four cases, the event happened in the afternoon, on October 23 (Sunday), October 26 (Wednesday), October 29 (Saturday), and October 30 (Sunday). Three of these four days were weekends. We cannot comment further on the relevance of the timing of these system-wide events. However, we can rather focus on characterizing the voltage waveform signatures of these 26 events; as we will discuss next.

### C. Analysis of System-Wide Damping Oscillations

Fig. 12 shows the scatter plot for the frequency of the oscillations at each of the 26 system-wide oscillatory events. Each point represents one event. Frequency extraction is done once at WMU 1 and once at WMU 2, by applying the Fourier Transform to the differential waveform of the event at each WMU, and recording the dominant frequency. The majority of the points in Fig. 12 are in the *diagonal* area. For these events, WMU 1 and WMU 2 extracted almost the same frequency. These system-wide events exhibited the same oscillations frequency at the waveforms that were *independently* captured by WMU 1 and WMU 2 at their respective locations.

As for the (only four) points that are in the *off-diagonal* area in Fig. 12, these are the cases where WMU 1 and WMU 2 extracted different frequencies. Two possibilities could account for the different frequencies at WMU 1 and WMU 2:

- **Possibility 1:** The true physical event manifested itself with different frequencies at these two different locations.

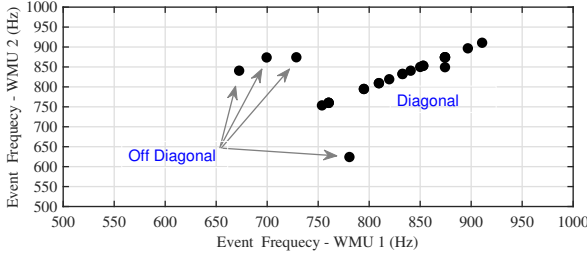


Fig. 12. Oscillation frequency for each system-wide oscillatory event based on frequency calculations at two locations, at WMU 1 and WMU 2.

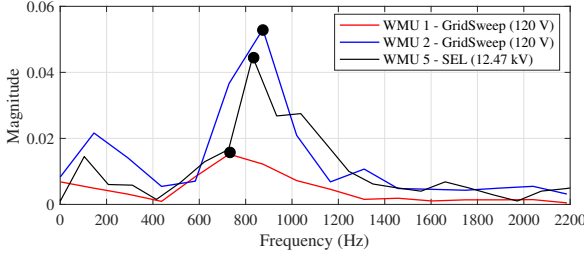


Fig. 13. The spectral analysis of the event signatures of the same system-wide event as it is obtained based on the event signatures at three different WMUs. The dominant frequency in each curve is marked with a black dot.

- **Possibility 2:** The true physical event manifested itself with the same frequency at these two locations; but the way that the measurements were collected resulted in observing two different frequencies at these two locations.

We cannot give a definitive determination on these possibilities. Nevertheless, it is insightful to also check these four (outlier) system-wide events also at the location of WMU 5, i.e., the three-phase SEL sensor at Substation 1. The results are shown for the case of one event in Fig. 13. Here, we show the spectral analysis of the event signatures of the exact same system-wide oscillatory event as it is captured by WMU 1 (GridSweep at 120 V), WMU 2 (GridSweep at 120 V), and WMU 5 (SEL at 12.47 kV). The dominant frequency of the oscillations is obtained at 728.6 Hz, 874.3 Hz, and 830.3 Hz by WMU 1, WMU 2, and WMU 5, respectively. Notice that the frequency that is extracted by WMU 5 is *between* the two frequencies that are extracted by WMU 1 and WMU 2. While this additional observation still does not lead to choosing between Possibility 1 and Possibility 2, it does yet again show the power of time-synchronized waveform measurements to detect and analyze various system-wide waveform events.

## VI. CONCLUSIONS

Data from continuous streaming of synchro-waveform measurements from four waveform sensors were analyzed over a period of one month, consisting a total of over 40 billion measurement samples. A method was proposed and tested for event detection. Several practical challenges were addressed, including the need to maintain light computational complexity due to the enormous amount of waveform data, the misalignment in the sampling points in relevance to the precise length of the waveform cycles, and the subtle challenges in extracting differential waveforms to reveal the event signatures. Examples of waveform events were presented and discussed,

including single-phase events and three-phase events. Furthermore, a series of system-wide events with oscillations were characterized by using data from two different locations that were supplied by two different utility substations. The analysis in this experimental study will shed light on the practical challenges in the new field of synchro-waveforms, specifically with respect to the sub-field of continuous streaming of synchro-waveforms from low-voltage circuits. This may prompt new avenues for further research in this area.

## ACKNOWLEDGEMENT

This work is supported in part by CEC grant EPC-16-077 through partial support of the graduate students who developed the methods to detect and analyze waveform events in power systems. GridSweep devices are developed by McEachern Laboratories through partial funding by the DOE, Office of Electricity and Office of Energy Efficiency Renewable Energy. The devices were loaned to UC Riverside for the experiments.

## REFERENCES

- [1] H. Mohsenian-Rad and W. Xu, "Synchro-waveforms: A window to the future of power systems data analytics," *IEEE Power and Energy Magazine* (accepted for publication), Apr. 2023.
- [2] A. F. Bastos, S. Santoso, W. Freitas, and W. Xu, "Synchrowaveform measurement units and applications," in *2019 IEEE Power Energy Society General Meeting (PESGM)*, 2019, pp. 1–5.
- [3] H. Mohsenian-Rad, *Smart Grid Sensors: Principles and Applications*. Cambridge University Press, UK, Apr. 2022.
- [4] J. Patterson and A. Pal, "An inductively powered line-mounted time-synchronized micro point-on-wave recorder," in *2021 IEEE Power Energy Society General Meeting (PESGM)*, 2021, pp. 1–5.
- [5] A. Shirsat, H. Sun, K. J. Kim, J. Guo, and D. Nikovski, "1 convnet: A convolutional energy disaggregation network using continuous point-on-wave measurements," in *2022 IEEE Power Energy Society General Meeting (PESGM)*, 2022, pp. 1–5.
- [6] A. McEachern and A. V. Meier, "An early report on active measurements of electric distribution grids," in *IEEE Power and Energy Society General Meeting (PESGM)*, Denver, CO, USA, Jul 2022.
- [7] A. McEachern, "GridSweep - New Instrument for Grid Stability Research," *NASPI Working Group Meeting*, Charlotte, NC, Oct. 2022.
- [8] B. Li, Y. Jing, and W. Xu, "A generic waveform abnormality detection method for utility equipment condition monitoring," *IEEE Trans. on Power Delivery*, vol. 32, no. 1, pp. 162–171, Feb 2016.
- [9] A. J. Wilson, D. R. Reising, R. W. Hay, R. C. Johnson, A. A. Karrar, and T. D. Loveless, "Automated identification of electrical disturbance waveforms within an operational smart power grid," *IEEE Trans. on Power Delivery*, vol. 11, no. 5, p. 4380–4389, Sep 2020.
- [10] M. R. Alam, F. Bai, R. Yan, and T. K. Saha, "Classification and visualization of power quality disturbance-events using space vector ellipse in complex plane," *IEEE Trans. on Power Delivery*, vol. 36, no. 3, p. 1380–1389, Jun 2021.
- [11] C. Ge, R. de Oliveira, I. Y.-H. Gu, and M. Bollen, "Deep feature clustering for seeking patterns in daily harmonic variations," *IEEE Trans. on Instrumentation and Measurement*, vol. 70, p. 1–10, Aug 2020.
- [12] D. Macii and D. Petri, "Rapid voltage change detection: Limits of the iec standard approach and possible solutions," *IEEE Trans. on Instrumentation & Measurement*, vol. 69, no. 2, p. 382–392, Feb 2019.
- [13] F. Ahmadi-Gorjaji and H. Mohsenian-Rad, "Data-driven models for sub-cycle dynamic response of inverter-based resources using wmu measurements," *IEEE Trans. on Smart Grid (early Access)*, May 2023.
- [14] M. Izadi and H. Mohsenian-Rad, "A synchronized lissajous-based method to detect and classify events in synchro-waveform measurements in power distribution networks," *IEEE Trans. on Smart Grid*, vol. 13, no. 3, pp. 2170–2184, May, 2022.
- [15] M. H. Bollen and I. Gu, *Signal Processing of Power Quality Disturbances*. John Wiley & Sons, 2006.
- [16] [Online] <https://www.mathworks.com/help/signal/ref/resample.html>.
- [17] A. McEachern, "Waveform apparatus disturbance detection and method," U.S. Patent 4,694,402, filed 1985, expired 2009.
- [18] [Online] <https://www.mathworks.com/help/matlab/ref/interp1.html>.